# Towards microalbuminuria determination on a disposable diagnostic microchip with integrated fluorescence detection based on thin-film organic light emitting diodes

Oliver Hofmann,[a] Xuhua Wang,[ab] John C. deMello,[c] Donal D. C. Bradley[b] and Andrew J. deMello*[c]

As a first step towards a fully disposable stand-alone diagnostic microchip for determination of urinary human serum albumin (HSA), we report the use of a thin-film organic light emitting diode (OLED) as an excitation source for microscale fluorescence detection. The OLED has a peak emission wavelength of 540 nm, is simple to fabricate on flexible or rigid substrates, and operates at drive voltages below 10 V. In a fluorescence assay, HSA is reacted with Albumin Blue 580, generating a strong emission at 620 nm when excited with the OLED. Filter-less discrimination between excitation light and generated fluorescence is achieved through an orthogonal detection geometry. When the assay is performed in 800 μm deep and 800 μm wide microchannels on a poly(dimethylsiloxane) (PDMS) microchip at flow rates of 20 μL min$^{-1}$, HSA concentrations down to 10 mg L$^{-1}$ can be detected with a linear range from 10 to 100 mg L$^{-1}$. This sensitivity is sufficient for the determination of microalbuminuria (MAU), an increased urinary albumin excretion indicative of renal disease (clinical cut-off levels: 15–40 mg L$^{-1}$)

## Introduction

Microalbuminuria (MAU) is defined as an increased urinary albumin excretion of 30–300 mg day$^{-1}$.[1] MAU is indicative of renal damage and predictive of incipient nephropathy in diabetic patients.[2] The American Diabetes Association thus recommends an annual MAU test for diabetics.[3] When detected at an early stage, MAU can be treated with reno-protective and anti-hypertensive therapy, prolonging the life of prospective patients.[4] Urine dipstick tests such as Micral® strips have been developed for MAU determination at the *point-of-care* (POC), *i.e.* in surgeries.[5] However, these semi-quantitative tests are normally used for initial screening only, followed by quantitative analysis in clinical laboratories.[6] Clinical testing is mainly based on nephelometric and turbidimetric immunoassays performed on bench top analysers. Immunoassay based tests exhibit excellent sensitivity, specificity and predictive value but current analyzers are costly and unsuitable for POC use.

Recently several groups have developed albumin tests in cartridge and microchip systems, including heterogeneous immuno-chromatographic assays,[7] homogenous immunoassays[8] and gel electrophoresis based separations.[9] Unfortunately these methods still rely on laser based fluorescence readers or spectrometers, and fluorescent labeling of either the detection antibody or albumin. Simpler dye binding assays have been developed by Kessler and co-workers.[10] The Albumin Blue 580 (AB 580) assay is based on a red-emitting fluorophore with specific affinity to albumin. Fluorescence quantum efficiency of AB 580 increases by two orders of magnitude upon binding to albumin. This fast and low-cost albumin assay has been successfully tested on a conventional fluorometer yielding detection limits for human serum albumin (HSA) of 1.4 mg L$^{-1}$, sufficiently below the 15–40 mg L$^{-1}$ cut-off limit for MAU.[11,12] Yager *et al.* applied this assay to a glass microchip and used a fluorescence microscope for detection. However, the assay was only used for evaluation of their T-sensor system and a limit of detection (LOD) was not determined.[13] In contrast, the presented work is aimed at performing the AB 580 assay on a disposable elastomer microchip for diagnostic applications[14] using an integratable low-cost thin-film organic light source for fluorescence detection.

In the Micro Total Analysis System (μTAS) and lab-on-a-chip (LOC) fields,[15–17] functional integration of optical components within monolithic substrates has only recently seen a spur of research and development efforts, as covered by some excellent reviews.[18–20] Inorganic light emitting diodes (LEDs)[21] have been employed as external light sources for on–chip absorbance[22] and fluorescence detection,[23,24] and also as integrated arrays for sensing applications.[25] Here for the first time we present the integration of organic light emitting diodes (OLEDs)[26] as an excitation source for the on-chip determination of MAU.

A typical OLED comprises one or more organic layers sandwiched between two electrodes. The organic layer emits light under electrical excitation *via* radiative recombination of injected electrons and holes. The emission characteristics are determined by the chemical structure of the organic material, and may therefore be controlled using standard synthetic chemistry. Most organic emitters are soluble, allowing for

[a]Molecular Vision Ltd., 90 Fetter Lane, London, EC4A 1JP, United Kingdom
[b]Department of Physics, Imperial College London, South Kensington, London, SW7 2AZ, United Kingdom
[c]Department of Chemistry, Imperial College London, South Kensington, London, SW7 2AZ, United Kingdom. E-mail: a.demello@imperial.ac.uk

low-cost deposition from solution, *e.g.* by inkjet printing. When fabricated on flexible substrates (*e.g.* PET films), reel-to-reel replication technology can be employed for mass manufacture. Owing to the simple design, OLEDs have great potential for integration into microfluidic systems at marginal additional cost. While the tuneable optical properties, simple fabrication, small size and low cost of OLEDs have attracted considerable interest in display technology for some time,[27–29] we have recently demonstrated their suitability as integrated excitation sources for microscale capillary electrophoresis.[30] Other groups have employed OLEDs as integrated light sources for glucose biosensors,[31] and for on-chip fluorescence spectroscopy.[32,33]

In the presented work OLEDs are successfully used as the light source for a diagnostic MAU microchip. Combined with the planned integration of organic photodiode detectors[34] and on-chip data display, this represents a promising pathway towards the realisation of fully integrated disposable diagnostic microchips for POC applications. In particular, these stand-alone credit-card sized devices are targeted at the low to medium volume home testing and doctor's surgery market, where a high upfront investment into cartridge/reader systems is not warranted.

## Experimental

### Microchip fabrication

The poly(dimethylesiloxane) (PDMS) microfluidic layers were fabricated by molding from an SU-8 master on a silicon substrate. Fabrication of the two-level SU-8 master was performed at the Centre of Integrated Photonics (Ipswich, UK) using standard SU-8 processing protocols. For PDMS molding a Sylgard 184 Silicone Elastomer kit (Dow Corning, Coventry, UK) was used. Monomer and hardener were mixed at a ratio of 10:1 w/w, degassed for 30 min and then poured over the SU-8 master. Three microscope cover slides were employed to define the side surfaces and top of the PDMS microfluidic layer being fabricated. While an optical grade side surface of the microfluidic layer is crucial for the orthogonal detection geometry we employed here, a flat upper surface is required for interfacing to the reservoir plate. After curing at 95 °C for 1 hour the microscope cover slides were removed and the ∼3 mm thick PDMS layer was pealed off. Access holes at the channel ends were punched with glass pasteur pipettes resulting in ∼2 mm diameter holes. To yield a more rigid microfluidic test device, a 1 mm thick microscope slide was used as the chip-to-world interface. Holes coinciding with the access holes in the PDMS microfluidic layer were drilled with a 1 mm diameter diamond drill bit. Standard fused silica capillaries (150 μm I.D., 367 μm O.D., Composite Metal Services, Hallow, UK) were then inserted and fixed with chemically resistant epoxy to serve as fluidic reservoirs (Araldite 2014, RS Components, Corby, UK). The PDMS microfluidic layer was reversibly attached to a chromium coated aperture plate with an opening coinciding with the detection chamber. The aperture plate was fabricated from glass plates coated with chromium and photoresist using standard photolithographic techniques (Nanofilm, Westlake Village, CA, USA).

The layout of the microalbuminuria determination microchip is shown schematically in Fig. 1. The device comprises two inlets, a meandering mixing channel, a detection chamber and an outlet. The inlets are 400 μm wide, 800 μm deep and 1 cm long, while the mixing channel is 800 μm wide, 800 μm deep and 5.2 cm long. The extended detection chamber is 5 mm long, 5 mm wide and 1.6 mm deep (volume 27 μL).

### Microfluidic system

For flow generation a PHD 2000 syringe pump (Harvard Apparatus, Edenbridge, UK) with 1 mL and 0.5 mL Bee Stinger gastight syringes (BAS, West Lafayette, In, USA) was employed. The syringes were connected to 1.6 mm I.D. high-pressure finger-tights (VWR, Poole, UK) *via* 762 μm I.D. PEEK tubing (Supelco, Bellefonte, PA, USA). The outlet of the finger-tights comprised 356 μm I.D. Teflon tubing (Anachem, Luton, UK) which could be connected to the capillary reservoirs of the PDMS microchip.

### Detection system

As an integratable excitation source a yellow thin-film OLED was employed in all experiments. The OLED was based on light emitting poly(p-phenylene vinylene) (PPV) derivative polymer, representative of present state of the art performance. The device structure typically comprised a patterned indium tin oxide (ITO) coated glass substrate onto which poly(3,4-ethylenedioxythiophene)/polystyrene sulfonate (PEDOT/PSS) was coated from aqueous solution (Baytron CH8000®, HC
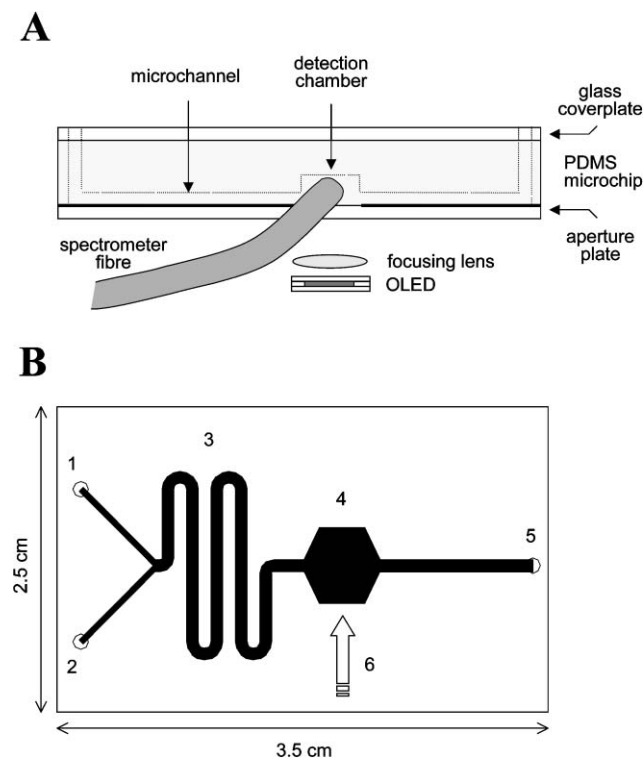


**Fig. 1** (A) Schematic of experimental set-up for microalbuminuria determination. (B) Microchip layout with inlets for AB 580 (1) and HSA (2), mixing channel (3), detection chamber (4), outlet (5) and orthogonal detection point (6).

Stark) to form a hole-injecting, anode layer. The PEDOT/PSS layer was baked at 120 °C for 30 minutes. The active PPV emission layer was spin-coated with a layer thickness of between 60 and 100 nm on top of PEDOT/PSS layer. The metal, electron-injecting, cathode was thermally evaporated on top, comprising a 5–20 Å LiF layer capped with a 150–200 nm layer of Al. The finished structure was encapsulated under inert gas in a glove box using a metal can and epoxy resin with desiccant to protect the active area of the device from moisture. As shown in Fig. 2 the OLED emission spans the wavelength range 500–700 nm with a maximum at 540 nm. The emission overlaps appreciably with the absorbance spectrum of the HSA/AB 580 complex, rendering the OLED an efficient excitation source. A Keithley 2400 Source Meter (Keithley Instruments, Reading, UK) was used as a constant current source for the measurements. The luminous intensity of the OLED emission was measured with an LS100 luminance meter (Minolta, Milton Keynes, UK). Focusing of the OLED output was achieved through a biconvex focusing lens. For orthogonal detection of complex emission a USB 2000 fibre optic spectrometer was employed (Ocean Optics, Duiven, The Netherlands). Data acquisition was performed through the USB port on a computer equipped with OOIIrrad software (Ocean Optics). The emission spectra were recorded using 5-scan averaging and a 200 ms integration time. Data smoothing and peak area determination was performed with Excel using standard methods.

### Albumin assay

All solutions were prepared from an Albumin Fluorescence Assay kit (Fluka Chemicals, Gillingham, UK) following the protocol provided in ref. 11. In short, AB 580 stock solution was diluted 1:50 v/v in buffer, resulting in ∼1.2 µM AB 580. Human serum albumin (HSA) was dissolved in calibrator solution. All solutions were refrigerated and used for a maximum of one week. To form the complex off-chip, AB 580 dye and HSA were mixed 5:1 v/v in a 2 mL Eppendorf vial, vortexed and then pumped through the microchip outlet at 50 µL min$^{-1}$. For complex formation on-chip, AB 580 and

HSA solutions were hydrodynamically pumped through microchip inlets 1 and 2, respectively, at a ratio of 2:1 v/v. For initial experiments 50 and 25 µl min$^{-1}$ were applied, resulting in a total flow rate of 75 µL min$^{-1}$. This was later reduced to 20 and 10 µL min$^{-1}$ or a total flow rate of 30 µL min$^{-1}$.

### Results and discussion

Initial experiments were focused on optimisation of detection efficiencies. The yellow OLED was current driven at 20–30 mA (7–8 V bias), yielding a brightness of 8,000 to 10,000 cd m$^{-2}$. While the OLED could be driven at a substantially higher bias at up to 50,000 cd m$^{-2}$ this severely limits its operational lifetime. To increase the excitation light density the OLED emission was focused onto the 5 mm × 5 mm detection chamber of the microfluidic chip. An aperture plate proved to be efficient in preventing excitation light scattering at the detection chamber sidewalls. To circumvent the need for a long pass emission filter, which would add to the complexity and cost of the targeted disposable diagnostic test, an orthogonal detection geometry was successfully implemented. For detection of HSA complex emission, the CCD spectrometer fiber was brought in close contact with the optical grade side surface of the PDMS microchip. Exact positioning of the fiber head proved to be crucial, with optimum results obtained with the fiber positioned just above the aperture plate and in the center of the detection chamber. Any mispositioning resulted in the detection of an unacceptably large contribution of scattered OLED light to the measured spectrum.

For first quantitation experiments HSA and AB 580 were mixed off-chip and then introduced in the microchip for detection. HSA concentrations in the range 1–1000 mg L$^{-1}$ were investigated, with water and AB 580 dye solutions serving as controls. While the presented experiments were conducted with aqueous HSA solutions, it should be noted that similar results would be expected for urine-based samples in MAU determination. Kessler et al. have shown that urine components such as proteins and drugs do not interfere with the AB 580 assay.[12] Fig. 3A depicts the smoothed data recorded with the CCD spectrometer. A general increase of the HSA/AB 580 complex emission peak at 620 nm can be observed for HSA concentrations above 30 mg L$^{-1}$. Interestingly the peak at 550 nm also shows variation that we attribute to movement of the optical fiber during the experiment. To facilitate interpretation of the data, Fig. 3B shows the same spectra normalised on the 550 nm peak. Normalised spectra reveal a discernible change of the complex emission peak for HSA concentrations as low as 10 mg L$^{-1}$. This is relative to the baseline emission of water and the weak emission of non-complexed AB 580.

Quantitation of normalised spectra was achieved through integration between 500 and 700 nm. The corresponding peak area as a function of the HSA concentration is depicted in Fig. 4A. A strong signal increase can be observed for lower HSA concentrations followed by leveling-off and signal saturation. This is due to the HSA/AB 580 complex formation obeying the mass action law and is in agreement with previously published quantitation data for HSA.[11–13] The
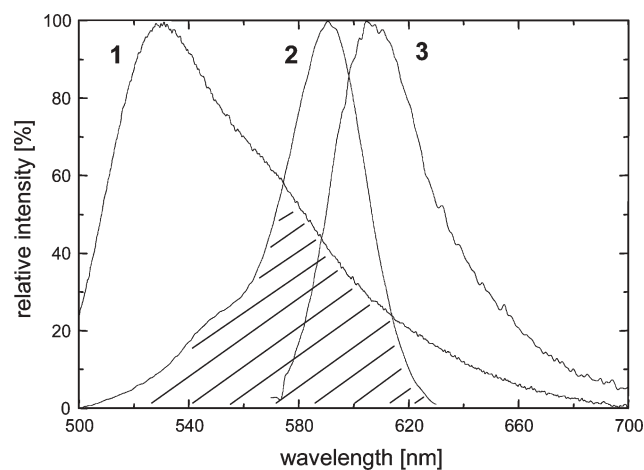


**Fig. 2** OLED emission spectrum (1) and overlap with excitation (2) and emission spectra (3) of 1.2 µM AB 580 dye after addition of 100 mg L$^{-1}$ HSA.
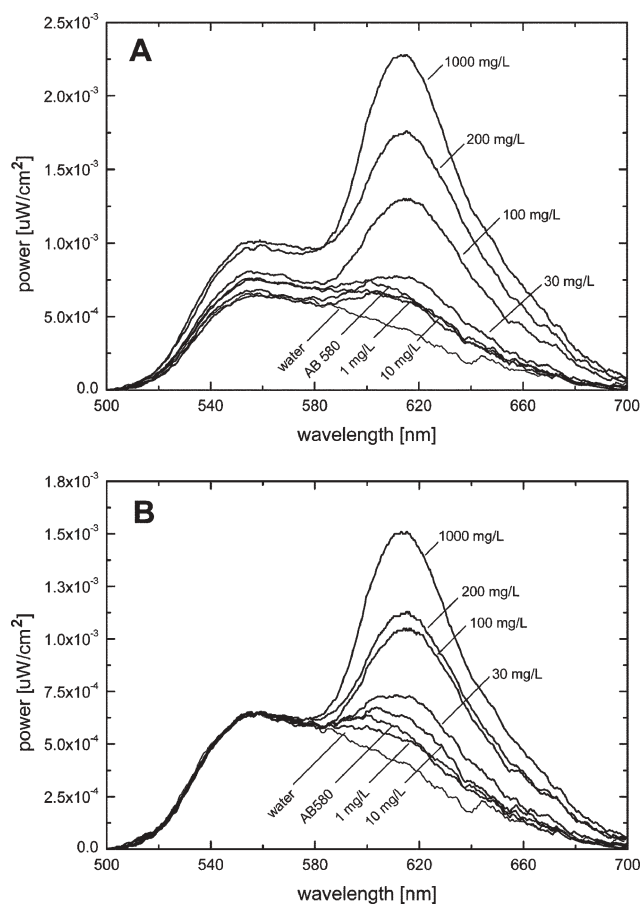
**Fig. 3** Detection of different HSA concentrations after mixing with 1.2 μM AB 580 dye. OLED driven at 20 mA. (A) Smoothed spectra. (B) Smoothed spectra normalised on peak at 550 nm.



**Fig. 4** HSA quantitation *via* peak area at 500 to 700 nm. Insets show linear range in diagnostically relevant HSA concentration range. Hatched area corresponds to 15–40 mg L$^{-1}$ cut-off limit for MAU. Limit of detection in both cases is ∼10 mg L$^{-1}$. (A) OLED driven at 20 mA. (B) OLED driven at 30 mA.

large excess of AB 580 employed in this assay accounts for the sharp increase in signal strength at low HSA concentrations. Linear regression analysis shows a linear range from 1–100 mg L$^{-1}$ HSA with a correlation coefficient, $R^2$, of 0.9923 (inset of Fig. 4A). However, given the threshold of 0.069 measured for the non-complexed dye control, only HSA concentrations of 10 mg L$^{-1}$ and higher can effectively be quantitated. Fig. 4B depicts HSA quantitation results obtained with the OLED driven at 30 mA. Overall the calibration curve follows the same trend as for 20 mA, but with higher 620 nm peak areas obtained over the entire concentration range. Again a linear range is observed from 1–100 mg L$^{-1}$ HSA, allowing for quantitation above 10 mg L$^{-1}$ (0.11 threshold value for AB 580). The apparent inability to enhance sensitivity through increasing light intensity points to a non-optimal detection alignment, *i.e.* detected excitation light and complex emission increase concurrently resulting in *no* discernible net-gain. Nevertheless the determined limit of detection (LOD) of 10 mg L$^{-1}$ HSA is clearly sufficient for the determination of MAU in clinical applications, with typical cut-off levels of 15–40 mg L$^{-1}$. Our detection limit compares to 1.4 mg L$^{-1}$ obtained in cuvettes on a conventional benchtop fluorometer.[12]

In subsequent experiments the effect of on-chip mixing on quantitation results was investigated. Initial experiments were conducted with flow rates of 25 and 50 μL min$^{-1}$ for HSA and

AB 580, respectively. While the detected signal intensities were generally in the same range as those for off-chip mixing, a signal increase was observed for the first ∼3 min after stopping the flow. This points to incomplete mixing due to an insufficient on-chip residence time of the reagents. Consequently the applied reagent flow rates were lowered to 10 and 20 μL min$^{-1}$, respectively. This completely negated any stopped flow effects, indicating complete intermixing of the two reagents. At the optimised flow rates an average on-chip residence time in the mixing channel and detection chamber of ∼120 s can be calculated. For AB 580 this results in a mean inter-diffusion distance of ∼350 μm, corresponding to approximately half channel width (based on a diffusion coefficient 5 × 10$^{-10}$ m$^2$ s$^{-1}$). It should be noted that in contrast to microwells and conventional vials, the employed microchip format not only provided efficient, potentially passive mixing but also facilitates the integration of planar organic detection components.

Adsorption of HSA inside the hydrophobic PDMS microchannels was subsequently investigated, since HSA loss to the channel walls could result in *false negatives* in MAU determination. Carry-over between runs was tested by first running the assay with high HSA concentrations followed by a

run with AB 580 only. Any HSA remaining in the microchannel should be complexed by the dye and thus be detectable as an increase in the complex emission peak at 620 nm. Between runs the microchannel was flushed with water for 10 min at 20 μL min$^{-1}$. As can be seen in Fig. 5, the recorded signals recover to baseline level, indicating negligible residual HSA in the microchannels after rinsing. While inter-run carry-over can be eliminated, some HSA adsorption during the assay is still likely to occur given the high affinity of hydrophobic proteins to PDMS. Interestingly this affinity of albumin to PDMS is exploited in microchip passivation protocols for immunoassays, where bovine serum albumin (BSA) concentrations up to 10 g L$^{-1}$ are used.[35] Recent studies on PDMS coatings, however, seem to suggest only limited BSA adsorption.[36]

While the presented results clearly demonstrate succesful HSA determination on a microchip, future efforts will focus on OLED device optimisation and more efficient coupling to the microchip. For diagnostic applications OLED batch-to-batch variations will be compensated for by measuring the luminescence/voltage characteristics and adjustment of the driving voltage. More efficient coupling could be achieved through size matching of OLED and detection chamber, microcavity OLEDs with narrow bandwidth emission,[37] or the use of integrated PDMS microlenses such as demonstrated by Camou *et al.*[38,39] Combined with organic photodiodes, such as previously applied to on-chip chemiluminescence detection,[40] and simple data display we now have the platform technology for a fully integrated stand-alone diagnostic MAU microchip. Given the reel-to-reel replication technology compatible low-cost fabrication of the microchip and detection components such disposable autonomous diagnostic devices hold great promise for the *point-of-care* market.[41]

## Conclusions

For the first time we have demonstrated the on-chip determination of HSA with a thin film OLED as the excitation source. Efficient mixing of HSA and AB 580 dye was performed in 800 μm wide and 800 μm deep microchannels on a molded PDMS microchip within 2 minutes. To circumvent the
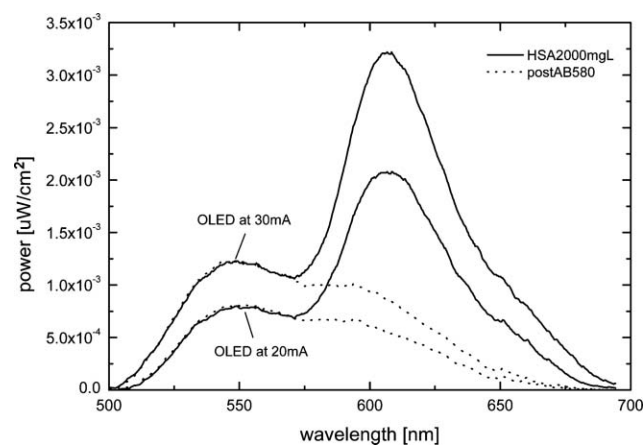
use of optical filters, an orthogonal detection geometry was successfully implemented using a microfluidic layer with optical-grade side surface. With a CCD spectrometer HSA/AB 580 complex formation was successfully monitored *via* the complex emission peak at 620 nm. Quantitation yielded a linear range between 10 and 100 mg L$^{-1}$ HSA and a 10 mg L$^{-1}$ limit of detection, sufficient for MAU determination. HSA loss due to non-specific adsorption on the hydrophobic PDMS microchannels was investigated, indicating minimal risk of *false negatives*. Although, in its current form the detection architecture is not fully integrated on chip, it still represents an important step towards the realisation of portable and disposable microfluidics based diagnostic tests. Both the microchip and OLED light source are easy to fabricate at low cost and considering passive filling, require only a battery for operation. In conjunction with similarly simple organic photodiode detectors and data display this could lead to fully disposable stand-alone diagnostic devices ideally suited for the *point-of-care* market.

## Acknowledgements

## References

1 *Microalbuminuria, a marker for organ damage*, ed. C. E. Mogensen, London Science Press, 1993.
2 J. L. Gross, M. J. de Azevedo, S. P. Silveiro, L. H. Canani, M. L. Caramori and T. Zelmanovitz, *Diabetes Care*, 2005, **28**, 164–176.
3 American Diabetes Association, *Diabetes Care*, 1995, **18**, Suppl. 1, 8–15.
4 C. E. Mogensen, W. F. Keane, P. H. Bennett, G. Jerums, H. H. Parving, P. Passa, M. W. Steffes, G. E. Striker and G. C. Viberti, *Lancet*, 1995, **346**, 1080–1084.
5 C. R. Parikh, M. J. Fischer, R. Estacio and R. W. Schrier, *Nephrol. Dial. Transplant.*, 2004, **19**, 2425–2425.
6 M. J. Pugia, J. F. Wallace, J. A. Lott, R. Sommer, K. E. Luke, Z. K. Shihabi, M. Sheehan and J. M. Bucksa, *J. Clin. Lab. Anal.*, 2001, **15**, 295–300.
7 S. Choi, E. Y. Choi, H. S. Kim and S. W. Oh, *Clin. Chem.*, 2004, **50**, 1052–1055.
8 Q. P. Qin, O. Peltola and K. Pettersson, *Clin. Chem.*, 2003, **49**, 1105–1113.
9 B. C. Giordano, L. J. Jin, A. J. Couch, J. P. Ferrance and J. P. Landers, *Anal. Chem.*, 2004, **76**, 4705–4714.
10 M. A. Kessler, M. R. Hubmann, B. A. Dremel and O. S. Wolfbeis, *Clin. Chem.*, 1992, **38**, 2089–2092.
11 M. A. Kessler, A. Meinitzer and O. S. Wolfbeis, *Anal. Biochem.*, 1997, **248**, 180–182.
12 M. A. Kessler, A. Meinitzer, W. Petek and O. S. Wolfbeis, *Clin. Chem.*, 1997, **43**, 996–1002.
13 A. E. Kamholz, B. H. Weigl, B. A. Finlayson and P. Yager, *Anal. Chem.*, 1999, **71**, 5340–5347.
14 E. Verpoorte, *Electrophoresis*, 2002, **23**, 677–712.

**Fig. 5** Evaluation of HSA carry-over. Between runs microchannels were rinsed with water at 20 μL min$^{-1}$ for 10 min.

15  D. R. Reyes, D. Iossifidis, P. A. Auroux and A. Manz, *Anal. Chem.*, 2002, **74**, 2623–2636.
16  P. A. Auroux, D. Iossifidis, D. R. Reyes and A. Manz, *Anal. Chem.*, 2002, **74**, 2637–2652.
17  T. Vilkner, D. Janasek and A. Manz, *Anal. Chem.*, 2004, **76**, 3373–3385.
18  J. C. Roulet, R. Volkel, H. P. Herzig, E. Verpoorte, N. F. de Rooij and R. Dandliker, *Anal. Chem.*, 2002, **74**, 3400–3407.
19  E. Verpoorte, *Lab Chip*, 2003, **3**, 42N–52N.
20  K. B. Mogensen, H. Klank and J. P. Kutter, *Electrophoresis*, 2004, **25**, 3498–3512.
21  P. K. Dasgupta, I. Y. Eom, K. J. Morris and J. Z. Li, *Anal. Chim. Acta*, 2003, **500**, 337–364.
22  G. E. Collins and Q. Lu, *Anal. Chim. Acta*, 2001, **436**, 181.
23  M. A. Burns, B. N. Johnson, S. N. Brahmasandra, K. Handique, J. R. Webster, M. Krishnan, T. S. Sammarco, P. M. Man, D. Jones, D. Heldsinger, C. H. Mastrangelo and D. T. Burke, *Science*, 1998, **282**, 484–487.
24  J. R. Webster, M. A. Burns, D. T. Burke and C. H. Mastrangelo, *Anal. Chem.*, 2001, **73**, 1622–1626.
25  E. J. Cho and F. V. Bright, *Anal. Chem.*, 2001, **73**, 3289.
26  A. Koehler, J. S. Wilson and R. H. Friend, *Adv. Engi. Mater.*, 2002, **4**, 453–459.
27  J. H. Burroughes, D. D. C. Bradley, A. R. Brown, R. N. Marks, K. Mackay, R. H. Friend, P. L. Burns and A. B. Holmes, *Nature*, 1990, **347**, 539–541.
28  R. H. Friend, R. W. Gymer, A. B. Holmes, J. H. Burroughes, R. N. Marks, C. Taliani, D. D. C. Bradley, D. A. Dos Santos, J. L. Bredas, M. Logdlund and W. R. Salaneck, *Nature*, 1999, **397**, 121–128.
29  D. Braun, *Mater. Today*, 2002, **June**, 32–39.
30  J. B. Edel, N. P. Beard, O. Hofmann, J. C. deMello, D. D. C. Bradley and A. J. deMello, *Lab Chip*, 2004, 4.
31  B. Choudhury, R. Shinar and J. Shinar, *J. Appl. Phys.*, 2004, **96**, 2949–2954.
32  S. Camou, M. Kitamura, J.-P. Gouy, H. Fujita, Y. Arakawa and T. Fujii, *Proc. SPIE*, 2002, **4833**, 1–8.
33  S. Camou, M. Kitamura, J.-P. Gouy, H. Fujita, Y. Arakawa and T. Fujii, in *Proceedings of Micro Total Analysis Systems (uTAS) 2002*, Kluwer Academic Publishers, Dordrecht; pp. 287–289.
34  O. Hofmann, A. J. deMello, D. D. C. Bradley, P. Miller and X. Wang, *G.I.T. Lab. J.*, 2004, **5**, 28–29.
35  O. Hofmann, G. Voirin, P. Niedermann and A. Manz, *Anal. Chem.*, 2002, **74**, 5243–5250.
36  S. L. Peterson, A. McDonald, P. L. Gourley and D. Y. Sasaki, *J.Biomed. Mater. Res. Part A*, 2005, **72A**, 10–18.
37  M. H. Lu and J. C. Sturm, *J. Appl. Phys.*, 2002, **91**, 595–604.
38  S. Camou, H. Fujita and T. Fujii, *Lab Chip*, 2003, **3**, 40–45.
39  J. Seo and L. P. Lee, *Sens. Actuators B—Chemical*, 2004, **99**, 615–622.
40  O. Hofmann, P. Miller, P. Sullivan, T. S. Jones, J. C. deMello, D. D. C. Bradley and A. J. deMello, *Sens. Actuators B—Chemical*, 2005, **106**, 878–884.
41  A. J. Tudos, G. A. J. Besselink and R. B. M. Schasfoort, *Lab Chip*, 2001, **1**, 83–95.